Supplemental Data

Supplemental Material and Methods

Supplemental Tables S1-8

Supplemental Figure Legends S1-10

Supplemental Figures S1-10

Supplemental Material and Methods

Clinical Samples

According to diagnostic frozen section analysis, a sample thought likely to be high grade epithelial (non-mucinous) OC was collected in medium and kept on ice (4^0C) for initial transportation (30-60 minutes). Roswell Park Memorial Institute (RPMI) 1640 medium was replaced with fresh medium containing 5% FCS. The tumor was cut into fragments (1-3 x 1-3 x 3 mm), which were then fixed in neutral buffered formalin (NBF) and paraformaldehyde (PFA), stored at 4^0C or snap frozen, stored at -80^0C or fixed in RNAlater solution (Invitrogen) and stored at 4^0C. Fragments for transplantation remained in medium containing 5% FCS at 4^0C. Formalin-fixed tissue was Paraffin Embedded and the block sectioned and stained using Haematoxylin and Eosin (H+E) for review by a Gynecologic Anatomical Pathologist.

Immunohistochemistry

Automated staining was performed with a Ventana BenchMark Ultra (Roche Diagnostics, USA). The slides were deparaffinized and incubated at 95°C for 36 min to enhance antigen retrieval and subsequently incubated with primary antibody at 37°C. The antibody was detected using UltraView Universal DAB detection kit (Roche Diagnostics). Slides were counterstained with Gills 2 haematoxylin (Australian Biostain). For Bcl-2 and Cyclin E1, antigen retrieval was performed in a high pH Ultra cell conditioning solution (CC1, Roche Diagnostics) for 64 min (Bcl-2) or 33 min (Cyclin E) at 96°C. Sections were incubated in the Bcl-2 antibody (clone 124, Dako) diluted at 1/25 for 32 min at 36°C or in Bcl-x_L antibody (clone 54H6, Cell Signaling). On-board detection using Amplification kit (amplifier B, Roche diagnostics) and UltraView Universal DAB detection kit (Roche Diagnostics) were used in accordance with the manufacturer's instructions. For Cyclin E, sections were incubated in the Cyclin E antibody (Clone 13A3, Thermo Scientific) diluted at 1/25 for 24 min at 36°C. On-board detection using

Amplification kit (amplifier B, Roche diagnostics) and OptiView Universal DAB detection kit (Roche Diagnostics) were used in accordance with the manufacturer's instructions.

qRT-PCR

Total RNA was extracted from snap frozen tumor material and RNAlater samples using the Qiagen AllPrep DNA/RNA/protein mini kit and 500 ng total RNA converted to cDNA using the Superscript III First-Strand Synthesis System (Invitrogen). For quantitative analysis, the resulting cDNA was diluted 1:2 with milliQ H_2O and 1.5ul was added to each qPCR 15 mL reaction volume using primers for *MYCN*, *LIN28B, LIN28A, HMGA2, CCNE1, HPRT* and, as an endogenous normalization control, *ACTB (β-actin)* (Primer sequences provided below) with SYBR-green reagent (Qiagen) and assessed on an ABI-PRISM 7900 thermal cycler (both from Applied Biosystems).

Generation of patient-derived xenografts (PDX).

Mice were anaesthetized by intra-peritoneal administration of ketamine (75 mg/kg) and xylazine (15 mg/kg) and with an analgesic (Carprofen, 10 mg/kg) delivered subcutaneously to control post-operative pain. The mouse was shaved over the right flank. Under anaesthesia, a small incision (>15mm) was made on the mouse's right flank, a subcutaneous pocket was made and a fragment of fresh tumor (1-3 mm x 1-3 mm x 3 mm) and/or a (contralateral) estrogen pellet (0.25 mg/pellet) was placed in the pocket. The skin was held together by autoclips. For the intra-ovarian bursal approach, under general anaesthetic, a small incision (>15 mm) was made in on the right flank of the mouse through the skin and into the peritoneum, exposing the ovary. A hole was made in the bursa and a fragment of tissue (>1 x 1 x 1mm) was placed inside. The body wall incision was closed by suture of the peritoneum and autoclips applied to the skin. Following surgery, animals received antibiotic, Fluoroquinolone *Baytril*®, in the drinking

water for 2 weeks and clips were removed 10 days post surgery. Recipient mice were monitored and noted for signs of loss-of-wellness including weight loss (more than 15% of body weight), body weight gain (more than 5 g with respect to age-matched non-tumorigenic controls), and for the presence of abdominal distension, respiratory distress, dehydration, anorexia, and/or diarrhea.

In vivo cisplatin treatments

Mice were weighed daily during therapy (days 1–18) and also if appearing unwell and at cull. No mice developed a significant change in weight (loss of more than 10% total body weight).

Western blotting

Protein samples were quantitated using the BCA assay (ThermoScientific). Protein samples were size-fractionated by SDS-PAGE and then blotted onto nitrocellulose (Invitrogen) membranes. The membranes were blocked with 10% non-fat dry milk (Devondale) in PBS with 0.1% Tween 20 (Sigma) and then probed with antibodies against Cyclin E (Clone HE12; Santa Cruz) and β-actin (clone AC-74, Sigma; also used as a loading control). Detection was performed with HRP-conjugated secondary antibodies and Enhanced Chemiluminescence (ECL) (Amersham Biosciences).

Real time qRT-PCR analysis primer sequences.

qRT-PCR was performed using the following forward and reverse primers:

Gene	sense (5' – 3')	antisense (5' – 3')
MYCN	CACAAGGCCCTCAGTACCTC	ACCACGTCGATTTCTTCCTC
LIN28B	TCTTCCAAAGGCCTTGAGTC	ATGATGATCAAGGCCACCAC
LIN28	AGGAAAGAGCATGCAGAAGC	GCTACCATATGGCTGATGCTC
HMGA2	ACTTCAGCCCAGGGACAAC	CTTGTTTTTGCTGCCTTTGG
CCNE1	GAAATGGCCAAAATCGACAG	TCTTTGTCAGGTGTGGGGA
HPRT1	GTTATGGCGACCCGCAG	ACCCTTTCCAAATCCTCAGC
ACTB	GCACAGAGCCTCGCCTT	GTTGTCGACGACGAGCG

Established Human HG-SOC Cell lines

As controls for qRT-PCR experiments, established human ovarian cancer cell lines were obtained, cultured and RNA made from cell pellets. OVCAR3 cells (*CCNE1* amplified) and SKOV3 cells were obtained from ATCC (a kind gift from D Huang).

Statistics

We presented the results we generated as descriptive analysis, categorising tumours for independent tests of phenotype. The data presented here demonstrate the variability within the cohort for various end-points analysed. These results can be used to generate hypotheses for further analyses in PDX studies.

Supplementary Table S1. Clinicosurgical characteristics of HG-SOC cohort.

Patient	Age	Menopausal Status	Primary site FT:Ovarian [d]	Se Ca125 U/mL	FIGO stage	Residual Disease	Family History	Mutation [e]
#5	51-60	Post	FT	100-400	IIIC	>15mm	Yes	*BRCA2*
#11	51-60	Post	Ovarian	100-400	IIIC	< 5mm	-	nmf
#13	51-60	Post	Ovarian	>4000	IIIC [f]	>15mm	Yes	*BRCA2*
#19	71-80	Post	Ovarian	100-400	IIIC	>15mm	Yes	*BRCA2*
#20	71-80	Post	FT	<35	IIIC	>15mm	-	nmf
#27	41-50	Pre	Ovarian	<35	IIIA	<15mm	-	nmf
#28	71-80	Post	Ovarian	100-400	IIC	< 5mm	Yes	*PMS2*
#29	81-90	Post	Ovarian	<35	IIIC	>15mm	-	nmf
#36	51-60	Post	Ovarian	400-1000	IIIC	< 5mm	-	nmf
#54	61-70	Post	FT	2000-4000	IIIC	< 5mm	-	*BRCA1*
#56	31-40	Pre	Ovarian	400-1000	IIIC	>15mm	-	*BRCA1*
#62	61-70	Post	FT	<35	IIC	nil	-	nmf
	63 [a], 61 [b] (38-89) [c]	2:10	4:8	<35: 4	IIIC: 9	>15mm: 7	BC/OC: 4	

Supplementary Table S1. Clinicosurgical characteristics of HG-SOC cohort. Clinical and surgical characteristics of the cohort of patients from whom HG-SOC fragments were transplanted were similar to previously published HG-SOC patient cohorts. Four women had Fallopian Tube cancer, two of which contained a DNA repair gene mutation. Four of six women who were found to have a HG-SOC containing a DNA repair gene reported a relevant family history. [a] mean, [b] median [c] range; [d] no primary peritoneal cancers

HG-SOC tumor; nmf – no mutation found in DNA repair genes (apart from in *TP53*); OC ovarian cancer, BC breast cancer, FIGO Federation of Gynecology and Obstetrics, surgical staging. [f] clinical staging.

Supplementary Table S2. *TP53* mutations identified by BROCA analysis.

HG SOC	TP53 IHC	Type	Mutation - GRCh37	Location[a]	Consequence	COSMIC Identifier
5	-	Deletion	Chr17:7578433-7578449 -:GACTGCTTGTAGATGG	c.482_497del16 p.A161fs*1	Frameshift	NA
11	+++	SNV	Chr17:7578257 C > A/A (A)	c.592G>T p.E198*	CDS Stop	COSM44241
13	-	Deletion	Chr17:7578184-7578193 -:GGCTCATAG	c.657_666delCTATGAGCC p.Y220_P222delYEP	Deletion	NA
19	+++	SNV	Chr17:7578467 T > G/G (G)	c.463A>C p.T155P	Missense	COSM10912
20	+++	SNV	Chr17:7578403 C > C/T (Y)	c.527G>A p.C176Y	Missense	COSM10687
27	+++	Insertion	Chr17:7578459-7578459 +:GAC	c.471_472insGAC p.V157_R158insC	In frame insertion	NA
28	+++	SNV/Indel	Chr17:7578416-7578417 CC > AA/CC (MM)	c.[513G>T;514G>T] p.[E171D;V172F]	Missense on same allele	NA
29	+++	SNV	Chr17:7577098 T > G/G (G)	c.804A>C p.R280S	Missense	COSM44233
36	+++	SNV	Chr17:7578190 T > C/T (Y)	c.659A>G p.Y220C	Missense	COSM10758
54	-	Deletion	Chr17:7578249 -:ATTTC	c.596_600delGAAAT p.G199fs*9	Frameshift	NA
56	+++	Deletion	Chr17:7576884-7576885 -:T	c.961delA p.K321fs*24	Frameshift	COSM44876
62	+++	SNV	Chr17:7578268 A > A/C (M)	c.581T>G p.L194R	Missense	COSM44571

Supplementary Table S2. *TP53* mutations identified by BROCA analysis. DNA was prepared from baseline HG-SOC and was analysed by massively parallel sequencing for mutations in DNA repair genes, including *TP53* (BROCA sequencing (Walsh et al., 2011)). A *TP53* mutation was found in each of the 12 HG-SOC. Presence of mutated p53 protein by IHC is shown. [a] Locations in TP53 reference sequence (Start codon = 1): NM_000546, NP_000537.

Supplementary Table S3. BROCAv4 assay sequencing targets.

Target Gene	**Target Region** (GRCh37)
APC	chr5:112038202-112186936
ATM	chr11:108088559-108244826
ATR	chr3:142163078-142303668
BABAM1 (BRCC45) (MERIT40)	chr19:17377232-17391162
BAP1	chr3:52430027-52449009
BARD1	chr2:215588275-215679428
BMPR1A	chr10:88511396-88689944
BRCA1	chr17:41191313-41282500
BRCA2	chr13:32884617-32978809
BRCC36	chrX:154298695-154352349
BRIP1	chr17:59754985-59945755
CDH1	chr16:68766195-68874444
CDK4	chr12:58137005-58151164
CDKN2A	chr9:21962751-21999490
CHEK1	chr11:125494031-125528042
CHEK2	chr22:29078731-29142822
FAM175A (ABRA1)	chr4:84381094-84407290
MLH1	chr3:37029979-37097337
MRE11A	chr11:94145467-94232040
MSH2 (+EPCAM)	chr2:47595263-47715360
MSH6	chr2:48005221-48039092
MUTYH	chr1:45789914-45811142
NBN	chr8:90940565-91001899
PALB2	chr16:23609483-23657678
PMS2	chr7:6007870-6053737
PRSS1	chr7:142452319-142465927
PTEN (+KILLIN)	chr10:89618195-89733532
RAD50	chr5:131887630-131984595
RAD51	chr15:40986378-41025356
RAD51B	chr14:68286496-69062738
RAD51C	chr17:56764963-56816692
RAD51D	chr17:33421811-33451888
RBBP8 (CTIP)	chr18:20512839-20607449
RET	chr10:43567517-43630795
SMAD4	chr18:48550583-48616409
STK11	chr19:1200798-1233434
TP53	chr17:7566720-7595863
TP53BP1	chr15:43698412-43803707
UIMC1 (RAP80)	chr5:176331006-176434780

VHL	chr3:10178319-10198744
XRCC2	chr7:152338589-152378250
XRCC3	chr14:104162954-104182823

Supplementary Table S3. BROCAv4 assay sequencing targets. List of genomic regions analysed by BROCA sequencing (Walsh et al., 2011), including DNA repair genes.

Supplementary Table S4. DNA repair gene mutations identified by BROCA analysis

HG SOC	Gene	Type	Mutation - GRCh37	Location [a]	Consequence	COSMIC Identifier
5	BRCA2	Insertion	Chr13:32913566-32913567 +:A	c.5073_5074insA p.K1691fs*3	Frameshift	NA
13	BRCA2	Deletion	Chr13:32914009-32914011 -:AG	c.5517_5518delAG p.V1839fs*6	Frameshift	NA
19	BRCA2	Deletion	Chr13:32910814-32910815 -:GGCTCATAG	c.2323delT p.S775fs*8	Frameshift	NA
28	PMS2	SNV	Chr7:6027135 G > A/G (R)	c.1261C>T p.R421*	CDS Stop	COSM179345
54	BRCA1	SNV	Chr17:41215948 G > A/G (R)	c.5095C>T p.R1699W [b]	Missense [b]	NA
56	BRCA1	Deletion	Chr17:41246652-41246654 -:AC	c.895_896delGT p.V299fs*3	Frameshift	NA

Supplementary Table S4. DNA repair gene mutations identified in baseline HG-SOC by BROCA analysis. DNA was prepared from baseline HG-SOC and was analysed by massively parallel sequencing for mutations in DNA repair genes (listed in Supplementary Table 3) other than *TP53* (reported in Supplementary Table 2). (BROCA sequencing (Walsh et al., 2011)). [a] Locations in reference sequences (Start codon = 1) BRCA1: NM_007294, NP_009225; BRCA2: NM_000059, NP_000050; PMS2: NM_000535, NP_000526. [b] known deleterious missense mutation (Easton et al., 2007).

Supplementary Table S5. Success rate of transplantation of baseline HG-SOC fragments.

HG-SOC	Subcutaneous N (%) (range)			Intrabursal[a] N (%) (range)		
	Recipient mice	PDX harvested	Days to harvest	Recipient mice	PDX harvested	Days to harvest
*BRCA1/2**						
#5	8	6 [b] (75)	140-207	ND		
#13	5	5 (100)	122-150	ND		
#19	6	1[b] (17)	124-183	3	1 (33)	159
#54	12	0 [c] (0)		6	1[c] (17)	159
#56	12	8 (67)	236-261	6	3 (50)	189-221
No mutation found (BROCA)						
#11	6	5 (83)	109-234	ND		
#20	6	0 (0)		6	0 (0)	
#27	6	3 (50)	110-291	6	1 (17)	219
#28	4	0 (0)		6	0 (0)	
#29	5	3 (60)	88-284	6	2 (33)	212-254
#36	6	3 (50)	181-249	6	5 (83)	195-276
#62	12	11 (92)	60-122	6	4 (67)	182-197

Supplementary Table S5. Success rate of transplantation of baseline HG-SOC fragments. HG-SOC fragments were transplanted into recipient mice and successful PDX-bearing mice were harvested at a tumor volume of 0.5-0.7 cm^3. **BRCA1* or *BRCA2* mutant HG-SOC; nmf - no mutation found by BROCA sequencing of 42 DNA repair genes (Walsh et al., 2011). Days to harvest. [a] murine ovarian bursa; [b] one additional recipient

identified with host-derived lymphoma; [c] multiple recipient mice were euthanased due to infection prior to tumor development.

Supplementary Table S6. Relative growth rates of independent HG-SOC PDX and median survival following cisplatin therapy

HG-SOC PDX	T1-3	Time to PD (d) cisplatin	Median TTH (d) vehicle	Median TTH (d) cisplatin	n (recipient mice)	p value for difference
Sensitive						
#5	T3	NA	60	undef	7, 13	< 0.0002
#11	T2	NA	28	155	4, 10	<0.0001
#11	T3	171	57	206	12, 11	<0.0001
#19	T2	NA	16	257	4, 4	<0.0177
#19	T3	247	15	undef	9, 11	<0.0001
#56	T2	120	36	undef	5, 8	0.0018
Resistant						
#13	T3	76	34	99	21, 13	<0.0001
#27	T2	62	30	118	4, 9	<0.0119
#54	T2	54	30	85	4, 4	0.0067
Refractory						
#29	T2	6	16	37	8, 14	<0.0001
#29	T3	3	19	29	4, 6	0.3704
#36	T2	22	22	48	11, 9	<0.0010
#62	T2	43	17	57	11, 13	<0.0001

Supplementary Table S6. Relative growth rates of independent PDX and median survival following cisplatin therapy. Recipient mice bearing T2 or T3 PDX were randomized to treatment with vehicle or cisplatin 4mg/kg, D1, 8, 18 when tumour volume reached 0.18-0.3 cm^3. Time to Progressive disease (PD) was defined as the time (in days) from beginning of cisplatin treatment to an increase in average tumor volume (for that treatment group) of >20% from the nadir (used to categorise PDX as sensitive (PD≥100

days), resistant (PD<100 days) or refractory to cisplatin). Time to Harvest (TTH) was defined as the time (in days) from the beginning of treatment to day of harvest at 0.7 cm^3 and the median TTH was calculated and plotted using Kaplan-Meier curves (Prism version 5). Control growth rates (treatment with vehicle) for independent PDX reveal that the slowest growth rates were observed for T3 of the most sensitive PDX, #5 and 11. As seen with the relatively early measure of time to PD, response to cisplatin was most durable for cisplatin-sensitive PDX, #5, 11, 19 (TTH > 150 d) and #56; intermediate for #13, 27 and 54 (cisplatin-resistant PDX; median TTH 99-118 d) and #29, 36 and 62 with median TTH of only 29-57 d (p value for difference between cisplatin and vehicle significant for all except #29 T3, indicating that two of three "refractory" PDX (#36 and #62) derived some short-term benefit from treatment). NA = Not Applicable as average PD was not reached. For the Kaplan Meier analysis of median TTH, mouse numbers were small beyond 150-200 days as some mice were euthanased due to age-related illness (common for this immune-deficient mouse strain).

Supplementary Table S7. Relative growth rates of independent mice bearing HG-SOC PDX undergoing re-treatment with second-line cisplatin therapy.

HG-SOC PDX (individual mouse)	Post 1st treatment to tumour volume 0.5 cm^3 (d)	Post 2nd treatment to tumour volume 0.5 cm^3 (d)
#13 (1)	109	61
#13 (2)	83	0#
#13 (3)	39	76
#13 (4)	79	38
#13 (5)	60	7
#13 (6)	106	10
#27 (1)	64	31
#27 (2)	67	40
#27 (3)	116	NA*

Supplementary Table S7. Relative growth rates of independent mice bearing HG-SOC PDX undergoing re-treatment with second-line cisplatin therapy. Recipient mice bearing PDX#13 or #27 were randomized to treatment with vehicle or cisplatin 4mg/kg, D1, 8, 18 when tumour volume reached 0.18-0.3 cm^3. Mice bearing recurrent PDX post cisplatin treatment were randomly allocated either to re-treatment with the same cisplatin regimen when the tumour volume reached 0.5 cm^3 in size or alternatively, tumor was harvested at 0.7 cm^3. Time to re-treatment for an individual mouse was defined as the time (in days) from the last day of treatment to first day of re-treatment (treatment free interval) for that mouse which occurred when tumour volume reached 0.5 cm^3. This was then compared with time from last day of re-treatment to the day when tumour volume for that mouse reached 0.5 cm^3. Re-treatment of a mouse with second-line cisplatin resulted in similar or shorter time in days for tumour volume to reach 0.5

cm^3, compared with the time taken following first-line treatment of that same mouse. At the time of re-treatment with second-line cisplatin, the tumour volume was larger than at time of first-line treatment, as is usually the case in the clinic (as most patients undergo primary but not secondary debulking surgery prior to platinum-based chemotherapy). d = days. NA* = mouse euthanased due to unrelated illness. $0^{\#}$ tumour failed to respond to second-line cisplatin (refractory).

Supplementary Table S8. T5a NGS Test platform analysis of PDX.

PDX #	*BRCA1/2* status	Other somatic mutations detected in addition to *TP53*	Other genetic alterations
5	*BRCA2*		ALK_amplification, NOTCH2_RCHY1_truncation
13	*BRCA2*	MAP2K1_c.167A>C	
19	*BRCA2*	NOTCH1_c.7192C>T, RB1_c.1164_1182del19	
54	*BRCA1*	LRP1B_c.381T>A	
56	*BRCA1*		RB1_intergenic region_truncation
11	*BRCA1* methylation*	MAP3K1_c.1842_1881del40, RB1_c.41_54del14, SMAD2_c.784+1G>T	
27	nmf		Homozygous del of RB1, Homozygous del of TSC1
29	nmf		Amplification of CCND2, CCNE1, EPHB1, FGF23, FGF6, KRAS, MCL1
36	nmf		Homozygous del of NF1 Amplification of MYST3 LRP1B_truncation
62	*BRCA1* methylation*		FGF12, NFKBIA, NKX2-1, and ZNF217 amplification CTNNA1_loss, EZH2_intergenicRegion_truncation

Supplementary Table S8. T5a NGS Test platform analysis of PDX. Foundation Medicine next generation sequencing (NGS) platform (T5a Test), which interrogates 287 genes as well as 47 introns of 19 genes involved in rearrangements. Additional mutations (likely to be somatic) detected were found in PDX containing mutations in either *BRCA1* or *BRCA2* or methylation of BRCA1. In contrast, all three refractory PDX were noted to have multiple other types of genetic aberrations, including oncogenic amplifications. The

deleterious mutations in *TP53* and either *BRCA1* or *BRCA2* were all confirmed. *BRCA1 methylation determined by bisulfite conversion and methylation-sensitive PCR.

Supplementary Figure S1. Histopathologic characteristics of HG-SOC and PDX.

Baseline HG-SOC and T3 PDX were stained by IHC for Estrogen Receptor, Progesterone Receptor p53, WT1 and PAX8. Relative expression between samples was similar for baseline HG-SOC and for PDX.

Supplementary Figure S2. Proliferative activity of HG-SOC and PDX.

IHC analysis of Ki67 for baseline HG-SOC and T1-3 PDX for #13, 29 and 62. Some selection was observed for Ki67 staining in PDX #13, however the pattern of staining was similar to that seen in the baseline sample across the cohort.

Supplementary Figure S3. Epithelial ovarian cancer PDX.

(A) Baseline HG-SOC #13, T1, T2 and T3 PDX #13 were stained by IHC for Estrogen Receptor, Progesterone Receptor p53, WT1 and PAX8. Relative expression between samples was similar for baseline HG-SOC and for PDX. (B) PDXs were stained with Haematoxylin and Eosin and also for the epithelial marker, pan-CK and for the pan-hemopoietic marker, CD45. T1 PDX which stained positively for pan-CK and negative for CD45 were considered to be epithelial in origin consistent with HG-SOC.

Supplementary Figure S4. Analysis of BRCA1 methylation in HG-SOC panel.

(A) DNA from fresh baseline HG-SOC and relevant control tumor samples were analysed for methylation of *BRCA1*. Baseline HG-SOC #11 and #62 were the only samples noted to contain methylation of *BRCA1*. (B) Baseline #11 and #62 (same DNA sample tested again) and multiple independent T2 and T3 PDX samples were analysed

(#11/1-4, #62/1-3). Presence of *BRCA1* methylation was stable and present in all #11 and #62 PDX tested. In PDX samples, unmethylated DNA may be less obvious because human stroma (which is likely responsible for that signal in the baseline samples) is replaced by mouse stroma (n=9 of each tested, n=3-4 of each shown).

Supplementary Figure S5. Response of cisplatin-resistant PDX.

Recipient mice bearing PDX from #27 and 54 were resistant to treatment with cisplatin. (A, E) Mean tumor volume (cm^3) following treatment with cisplatin, (B, F) responses for individual mice. Recipient mice bearing T2 PDX were randomized to treatment with vehicle or cisplatin 4 mg/kg, D1, 8, 18. Tumor measurements were monitored up to three times per week. PDX were harvested at a tumor volume of 0.7 cm^3 or re-treated with the same regimen at 0.5 cm^3. During *in vivo* treatment with three doses of cisplatin, PDX #27 and 54 ^{BRCA2} T2 underwent initial tumor regression, however, this was followed by PD (defined as 20% increase in tumor volume compared with nadir) at 62 and 54 d respectively (see Supplementary Table S6 for median time to harvest and p values for difference). Mice bearing recurrent tumours were randomly allocated either to (C) re-treatment with the same cisplatin regimen as before, when the tumour volume reached 0.5 cm^3 ("re-treated 2nd-line") or (D) tumor was harvested at 0.7 cm^3, transplanted and recipient mice were treated with vehicle or cisplatin ("transplanted 2nd-line"). Coloured asterixes in (B) correspond to coloured line in (C). Error bars represent Standard Deviation (SD), n= individual mice.

Supplementary Figure S6. Cisplatin sensitivity for HG-SOC PDX across the cohort.

Recipient mice bearing PDX at serial transplantation stage T2 or T3 were randomized to treatment with vehicle or cisplatin 4mg/kg, D1, 8, 18. Data are shown for individual mice. Responses are shown for independent PDX, from most cisplatin sensitive (PDX #19) to most cisplatin refractory (PDX #29, see Supplementary Table S6 for median time to harvest and p values for difference; For PDX #54, refer to Supplementary Figure S5).

Supplementary Figure S7. Stable cisplatin response phenotype in serial HG-SOC PDX.

Recipient mice bearing PDX at serial transplantation stage T2 or T3 or T4 were randomized to treatment with vehicle or cisplatin 4 mg/kg, D1, 8, 18. Mean tumor volume (cm^3) following treatment with cisplatin. Responses to cisplatin were similar for serial PDX. (A-C) PDX #11 (cisplatin sensitive) T2 versus T3 versus T4; (D-E) PDX #19 (cisplatin sensitive) T2 versus T3; (F-G) PDX #13 (cisplatin resistant) T2 versus T3; (H-I) PDX #29 (cisplatin refractory) T2 versus T3 (see Supplementary Table S6 for median time to harvest and p values for difference). Error bars represent Standard Deviation (SD), n= individual mice.

Supplementary Figure S8. qRT-PCR analysis of the MYCN pathway and *CCNE1* in baseline HG-SO and PDX.

Analysis of baseline HG-SOC by qRT-PCR for *mRNA* expression of the MYCN pathway and *CCNE1*. (A) *MYCN* levels were high in HG-SOC #20 and 29 (all samples normalized to CH1). (B) *LIN28B* levels were high in HG-SOC #29 and #36 (all samples normalized

to CH1). (C) *CCNE1* expression was high in HG-SOC #29. HG-SOC #62 had the next highest level of *CCNE1*, consistent with heterogenous high expression by IHC (Supplementary Figure S8) (all samples normalized to SKOV3). Dotted line indicates level of positive control cell lines: CH1, increased expression of *MYCN* (Helland et al., 2011), OVCAR3, amplified for *CCNE1*(Etemadmoghadam et al., 2010). SKOV3 cell line, not amplified for *CCNE1*. qRT-PCR average of 3-7 experiments (one baseline RNA sample per HG-SOC). Error bars represent Standard Deviation (SD).

Supplementary Figure S9. Expression of Bcl-2 and Cyclin E in HG-SOC.

(A-C) Bcl-2 and Cyclin E expression by IHC in baseline HG-SOC. (A) HG-SOC with low, medium or high staining for Bcl-2. (B) HG-SOC with low or high staining for Cyclin E. HG-SOC #62 had areas of tumor with high staining for Cyclin E and areas of low staining. In contrast, all areas of #29 stained strongly for Cyclin E. (C) Quantification of protein expression as assessed by IHC. Line at score 150 indicates cut-off for HG-SOC hypothesized to have higher levels of expression. (D) Western blotting of Cyclin E in PDX. Highest expression was observed in PDX #29 and 62. Positive control cell line (run on same gel): OVCAR3, amplified for *CCNE1* (Etemadmoghadam et al., 2010).

Supplementary Figure S10. Expression of Cyclin E in PDX #62 following treatment with cisplatin.

Mice bearing different aliquots of PDX #62 were treated with cisplatin and response to treatment was observed. Mice with the shortest response time to cisplatin had aliquots of

PDX #62 with the highest level of *CCNE1* expression as analysed by qRT-PCR, r-squared value 0.6163 (60% of the variance of the means explained by fold change of *CCNE1* expression), slope (95% CI) -31.29 (-53.35 to -9.222).

References

Easton, D.F., Deffenbaugh, A.M., Pruss, D., Frye, C., Wenstrup, R.J., Allen-Brady, K., Tavtigian, S.V., Monteiro, A.N., Iversen, E.S., Couch, F.J.*, et al.* (2007). A systematic genetic assessment of 1,433 sequence variants of unknown clinical significance in the BRCA1 and BRCA2 breast cancer-predisposition genes. American journal of human genetics *81*, 873-883.

Etemadmoghadam, D., George, J., Cowin, P.A., Cullinane, C., Kansara, M., Gorringe, K.L., Smyth, G.K., and Bowtell, D.D. (2010). Amplicon-dependent CCNE1 expression is critical for clonogenic survival after cisplatin treatment and is correlated with 20q11 gain in ovarian cancer. PloS one *5*, e15498.

Helland, A., Anglesio, M.S., George, J., Cowin, P.A., Johnstone, C.N., House, C.M., Sheppard, K.E., Etemadmoghadam, D., Melnyk, N., Rustgi, A.K.*, et al.* (2011). Deregulation of MYCN, LIN28B and LET7 in a molecular subtype of aggressive high-grade serous ovarian cancers. PloS one *6*, e18064.

Walsh, T., Casadei, S., Lee, M.K., Pennil, C.C., Nord, A.S., Thornton, A.M., Roeb, W., Agnew, K.J., Stray, S.M., Wickramanayake, A.*, et al.* (2011). Mutations in 12 genes for inherited ovarian, fallopian tube, and peritoneal carcinoma identified by massively parallel sequencing. Proceedings of the National Academy of Sciences of the United States of America.

Topp_Supp_Fig_1

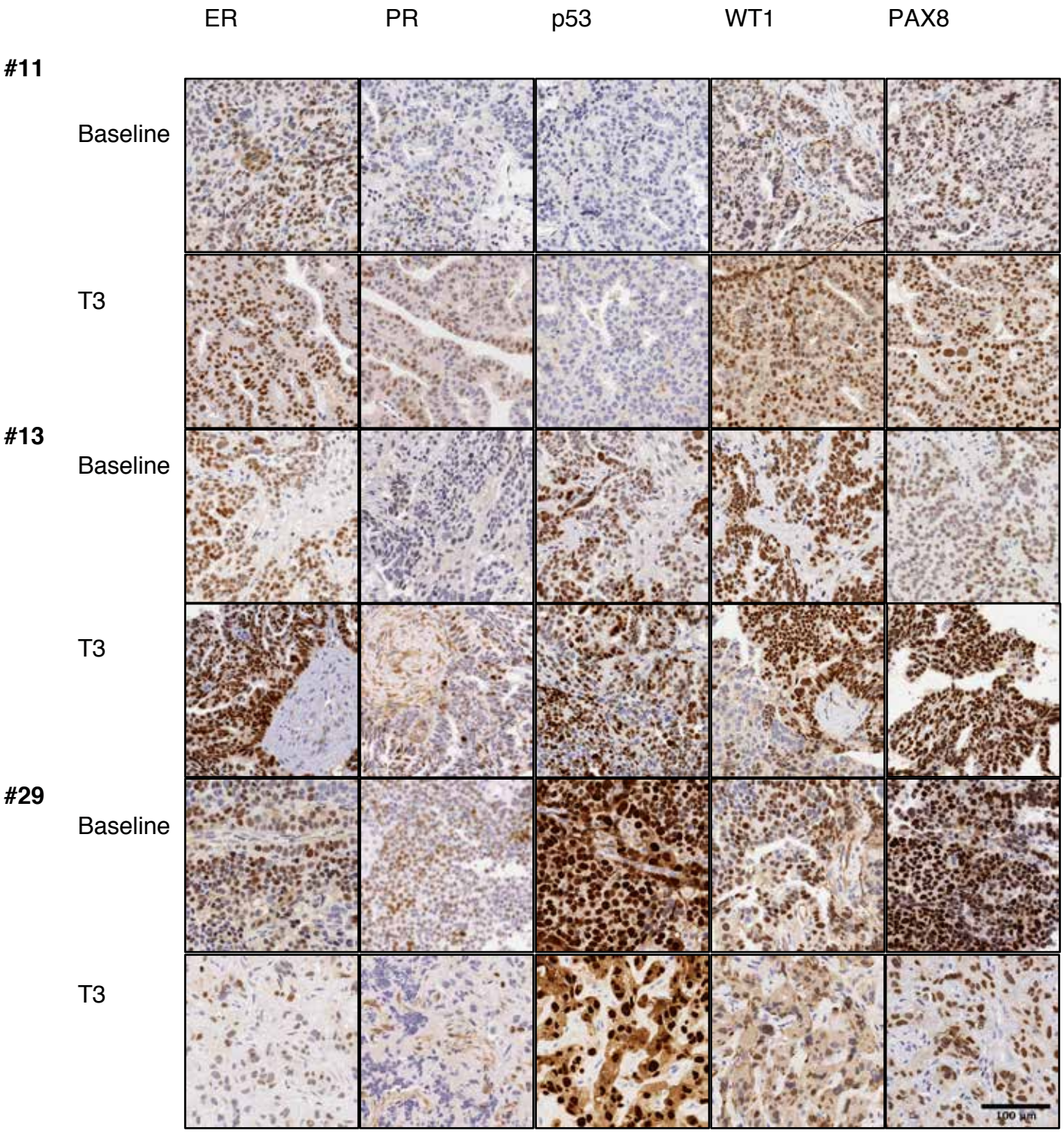

Topp_Supp_Fig_2

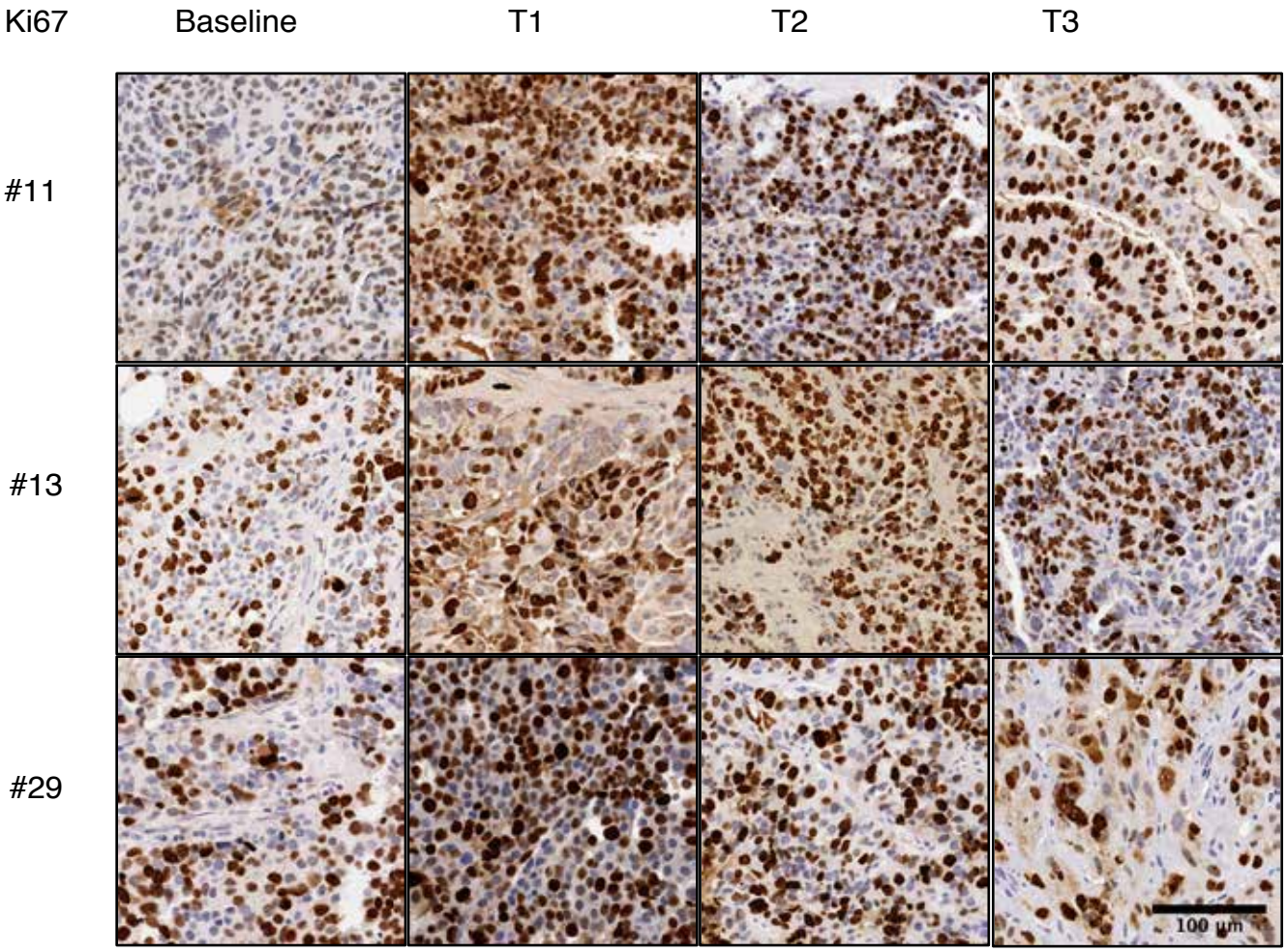

Topp_Supp_Fig_3

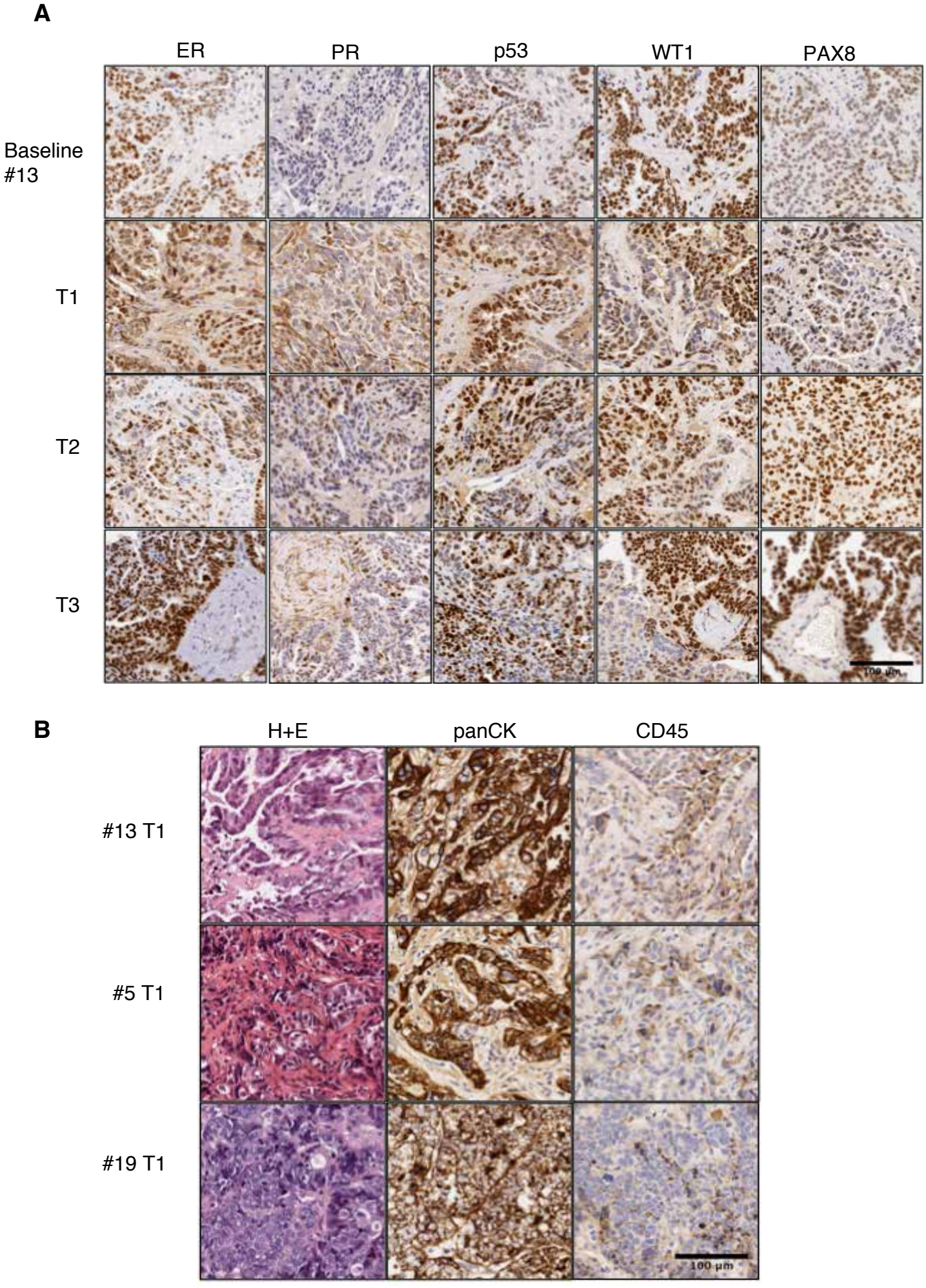

A

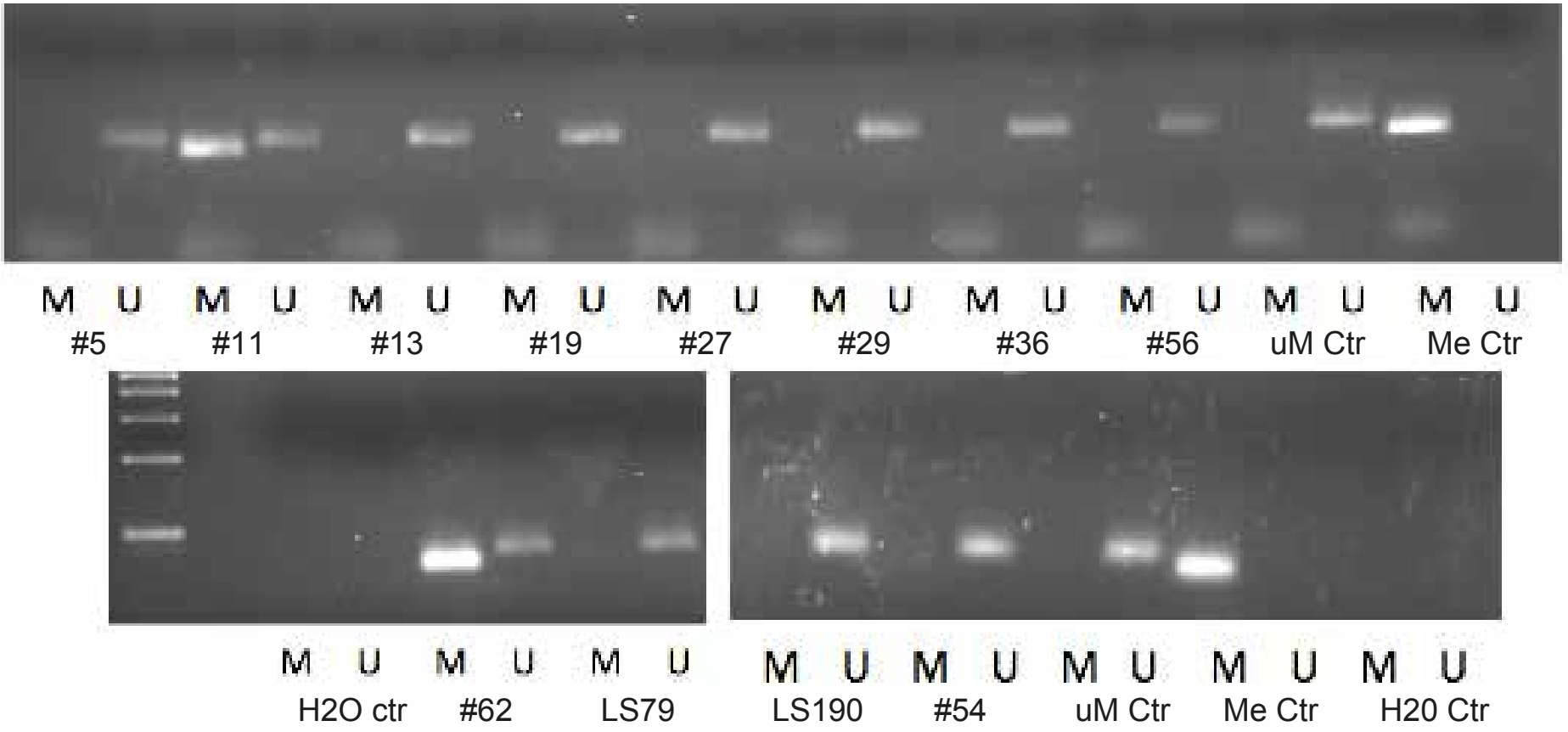
M U M U M U M U M U M U M U M U M U M U
#5 #11 #13 #19 #27 #29 #36 #56 uM Ctr Me Ctr
M U M U M U
H2O ctr #62 LS79
M U M U M U M U M U
LS190 #54 uM Ctr Me Ctr H20 Ctr

B

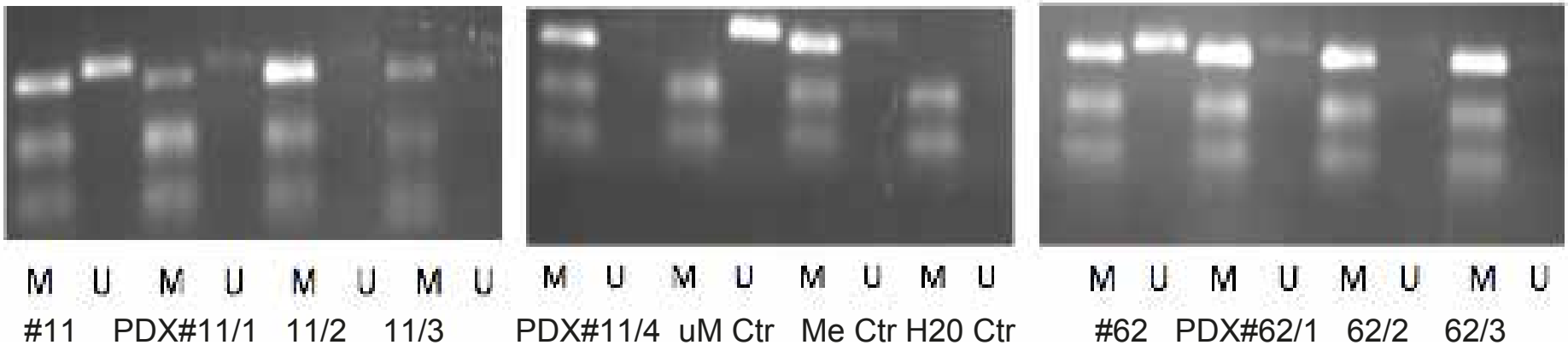
M U M U M U M U
#11 PDX#11/1 11/2 11/3
M U M U M U M U
PDX#11/4 uM Ctr Me Ctr H20 Ctr
M U M U M U M U
#62 PDX#62/1 62/2 62/3

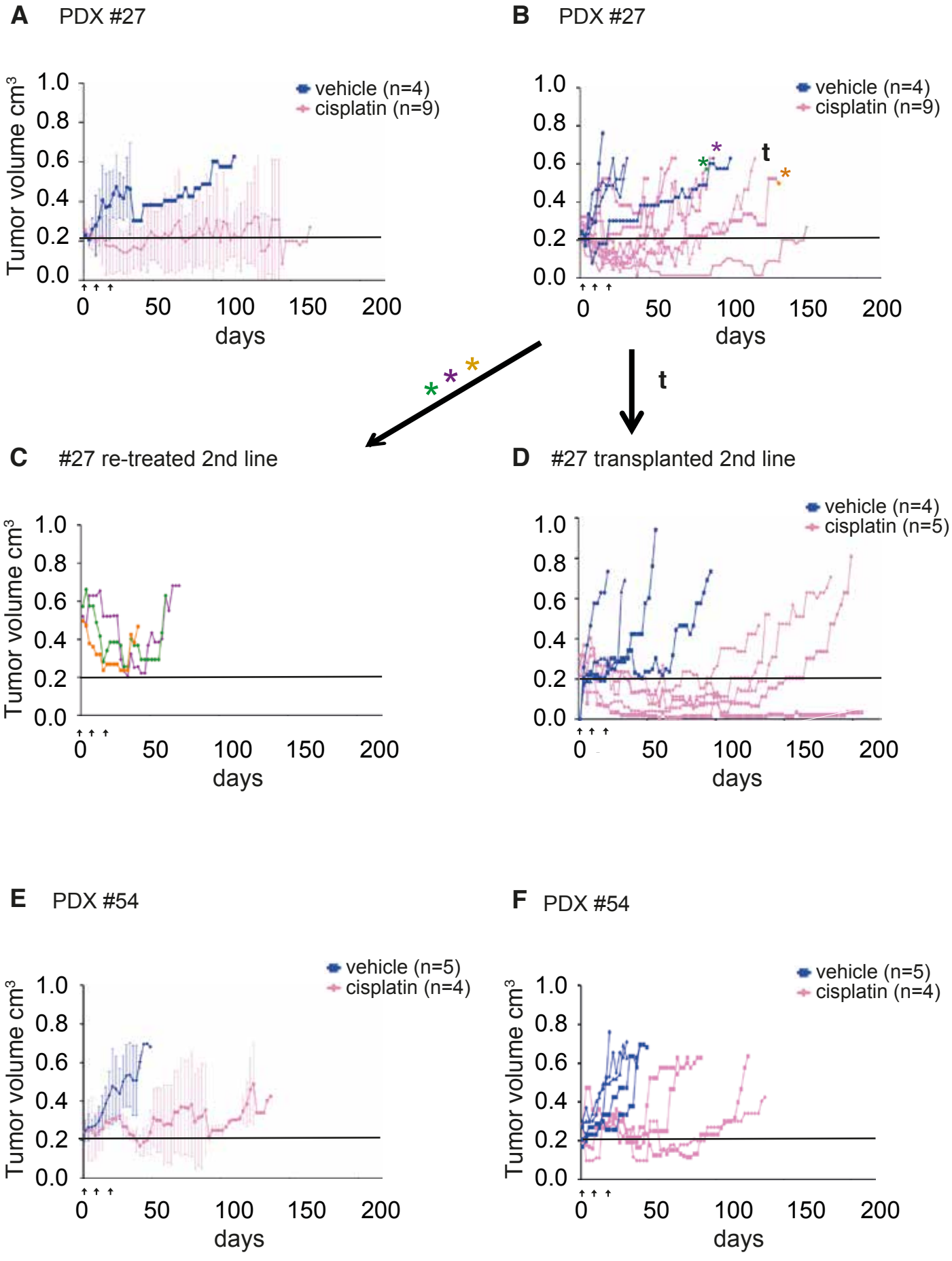
A
PDX #27
B
PDX #27
vehicle (n=4)
cisplatin (n=9)
Tumor volume cm³
1.0
0.8
0.6
0.4
0.2
0.0
0
50
100
150
200
days
t
C
#27 re-treated 2nd line
D
#27 transplanted 2nd line
vehicle (n=4)
cisplatin (n=5)
E
PDX #54
F
PDX #54
vehicle (n=5)
cisplatin (n=4)

Topp_Supp_Fig_6

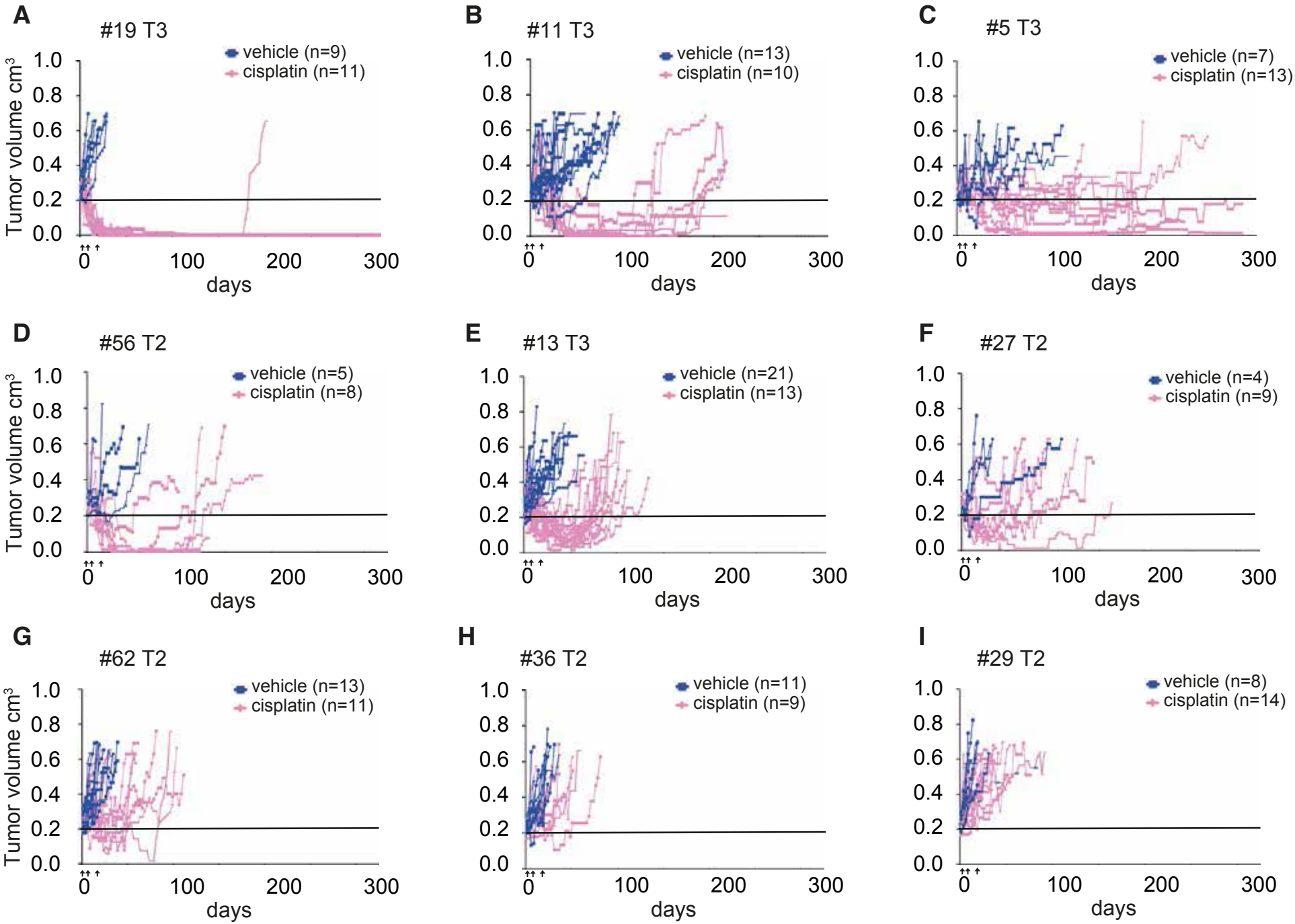

Topp_Supp_Fig_7

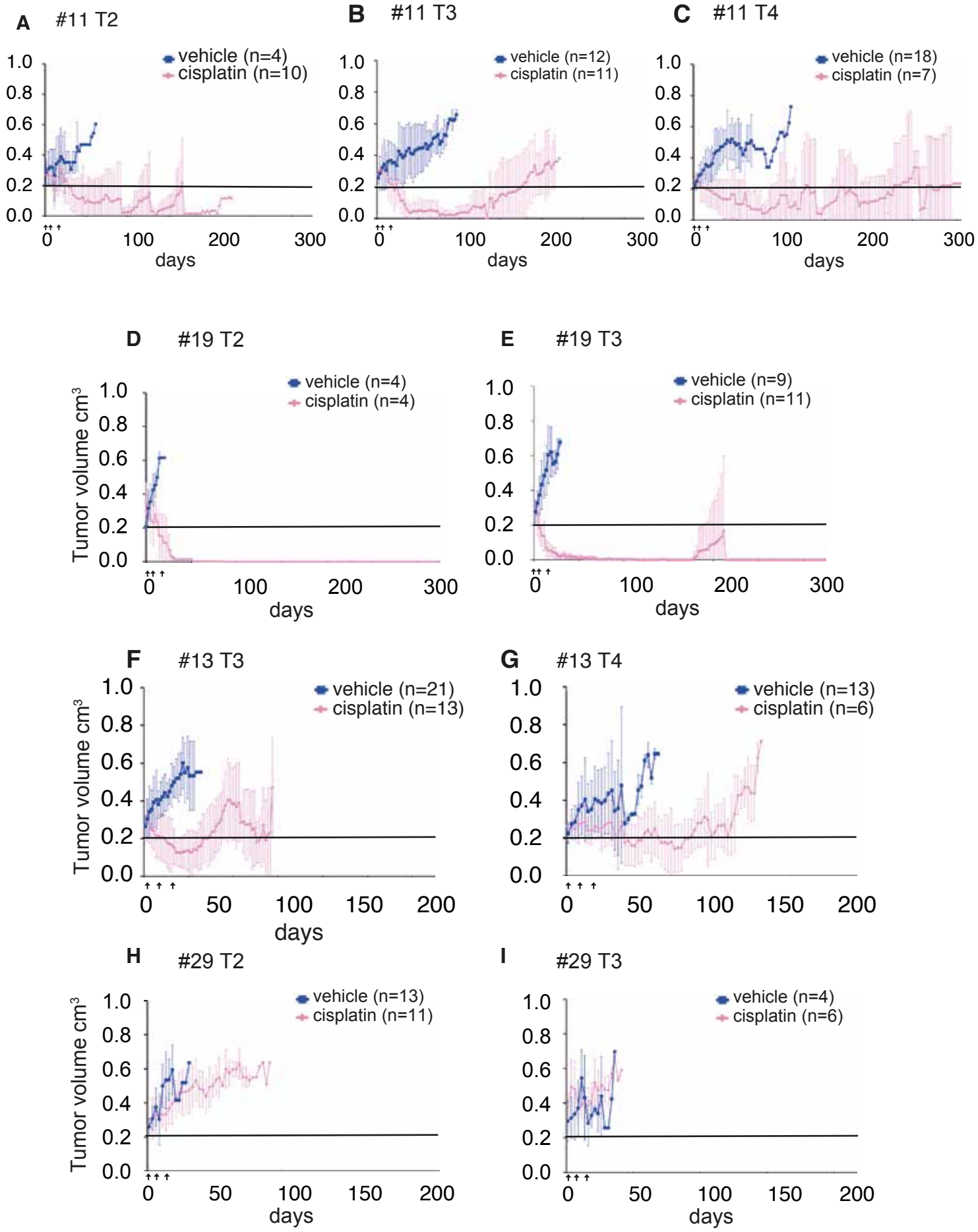

Topp_Supp_Fig_8

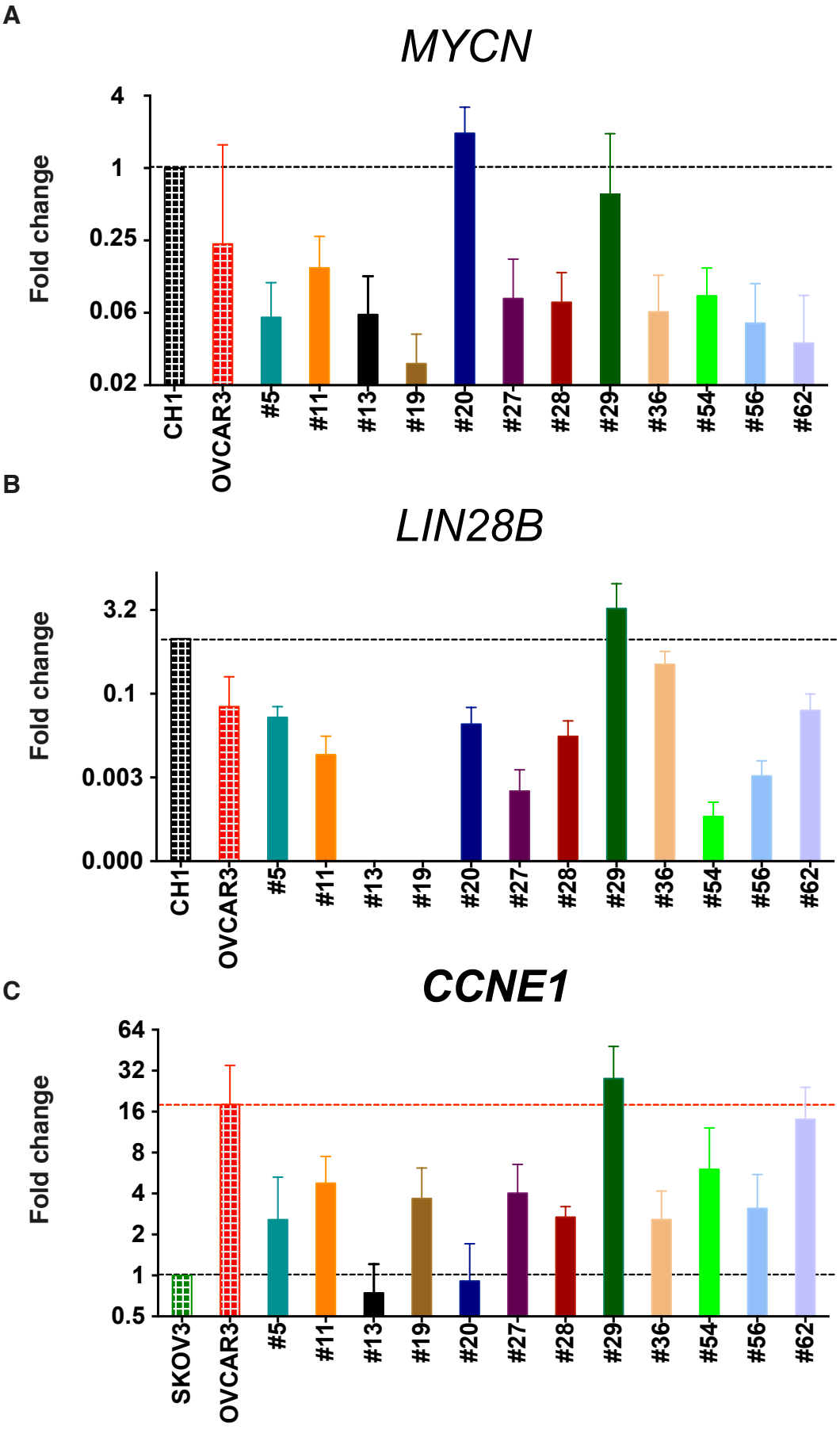

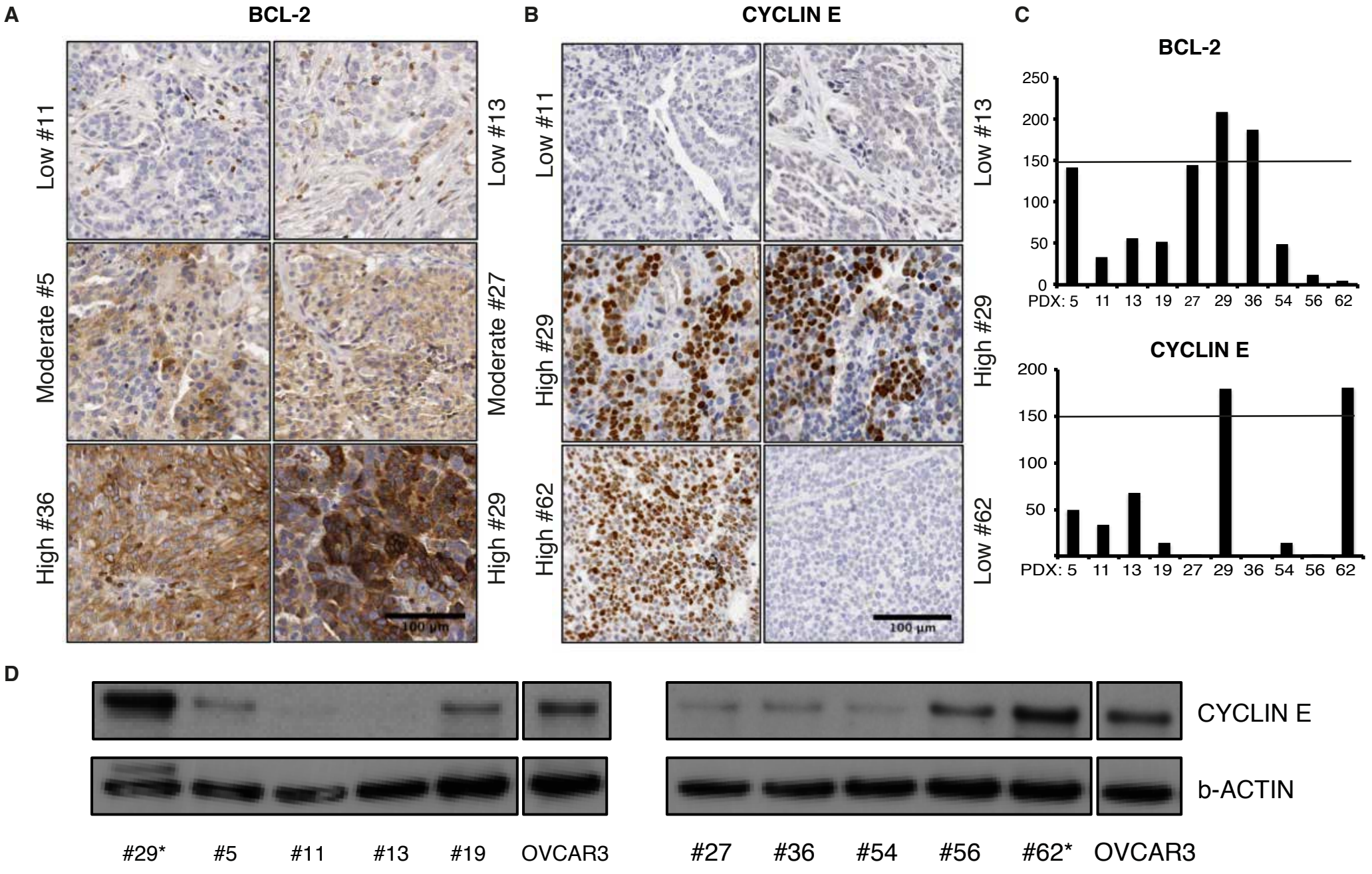
A
BCL-2
Low #11
Low #13
Moderate #5
Moderate #27
High #36
High #29
100 µm
B
CYCLIN E
Low #11
Low #13
High #29
High #29
High #62
Low #62
100 µm
C
BCL-2
250
200
150
100
50
0
PDX: 5 11 13 19 27 29 36 54 56 62
CYCLIN E
200
150
100
50
PDX: 5 11 13 19 27 29 36 54 56 62
D
CYCLIN E
b-ACTIN
#29* #5 #11 #13 #19 OVCAR3
#27 #36 #54 #56 #62* OVCAR3

Topp_Supp_Fig_10